Nuclear Data for Science and Technology (1988 MITO), 311- 314, Copyright © 1988 JAERI.

MEASUREMENTS OF DISCRETE GAMMA-RAY PRODUCTION CROSS SECTIONS FOR THE INTERACTIONS OF 14.9MeV NEUTRONS WITH COBALT*

Zhou Hongyu, Tang Lin, Fan Guoying, Yan Yiming, Sun Suxu, Wang Qi, Lan Liqiao, Wen Chenlin, Hua Ming, Liu Shuzhen, Rong Yaning and Yan Hua

Institute of Low Energy Nuclear Physics
Beijing Normal University, Beijing, China

Abstract: Differential production cross sections for 63 discrete gamma-rays from 14.9MeV neutron induced $^{59}Co(n,x\gamma)$ reactions were measured with a Ge(Le) detector at 30° to 140°. The pulsed-beam time-of-flight technique was employed for background reduction. probable reaction types and transitions of the better part of gamma-ray lines were assigned. Neutron inelastic scattering cross sections for 10 levels and total neutron inelastic scattering cross section of ^{59}Co in 14.9MeV incident neutron energy were obtained.

(nuclear reaction, cobalt, 14.9MeV neutron, pulsed-beam time-of-flight technique, discrete gamma-ray production cross section, neutron inelastic scattering cross section)

Introduction

The researches of associated gamma-ray spectra and production cross sections from fast neutron induced nuclear reactions not only have been a powerful tool of studying nuclear strutures and nuclear reaction mechanism, but also can provide useful nuclear data for nuclear engineerings and nuclear technology applications. Cobalt is an important constituent of ferrous alloys which are used as structural materials in reactor and other installations where fast neutrons abound. Its energy level and decay scheme are also of interest from a basic physics point of view. In the incident neutron energy range 1 to 5MeV a lot of measurements of gamma-ray spectra and production cross sections for $^{59}Co(n,n'\gamma)^{59}Co$ reactions have been made[1-4], which ever played an important part in establishment of energy level and decay scheme in ^{59}Co.

In recent years the developments of fusion reactors require to obtain gamma-ray production cross section and neutron inelastic scattering cross section data in higher incident neutron energy. But only V. Corcalcivc[5] measured a part of gamma-ray production cross section data from $^{59}Co(n,x\gamma)$ reaction in the incident neutron energy range 16.2 to 21.8MeV so far, in which only 22 gamma-ray lines were determined and there appear larger systematic errors in obtained cross section data.

In present work discrete gamma-ray spectra for $^{59}Co(n,x\gamma)$ reactions in 14.9MeV incident neutron energy were measured respectively at 7 angles between 30° and 140° to the incident neutron direction. Differential cross sections and angular distributions of 63 individual gamma-ray lines are determined, probable reaction types and transitions of the better part of the gamma-ray lines were assigned, as well as neutron inelastic scattering cross sections for 10 levels and total neutron inelastic scattering cross section of ^{59}Co in 14.9MeV incident neutron energy were obtained.

Experimental Methods

The experimental arrangement is shown in Fig.1. The experiments were carried out at a pulsed neutron time-of-flight facility based on a 400KV Cockcroft Walton accelerator. Monoenergetic 14.9MeV neutrons were obtained from $T(d,n)^4He$ reactions using 300keV pulsed deuteron and a solid T-Ti target. The repetition frequency of pulsed beams was 3.16MHz. The FWHM of pulses was 1 ns or so. Averaged deuteron beam current was 4 μa, and averaged neutron intensity was about 5×10^8/sec. The neutron flux incident upon the

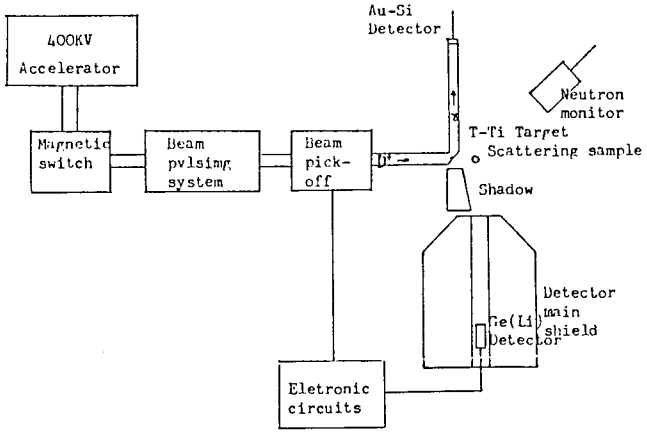

Fig. 1 General view of the experimental set-up

sample was determined by associated alpha particle counting with a Au-Si detector. The cobalt sample is a solid cylinder in 3cm diameter and 3cm high, the purity of which is more than 99.9%. The sample was placed on the deuteron beam axis direction and at 13.4cm from the neutron target.

The gamma-ray spectra from $^{59}Co(n,x\gamma)$ reactions were detected by the coxial Ge(Li) detector which was placed in a heavy shield. Its full energy peak efficiency curve from 26keV to 10.8 MeV, and single and double escape peak efficiency curves from 1.77 to 10.8MeV (Fig.2) were obtained by means of 7 standard gamma-ray sources and 6 multiline gamma-ray sources with known relative intensities.

The pulsed-beam time-of-flight technique was employed to reduce background caused by primary and scattered neutrons. The time spectrum of the pulses in the Ge(Li) detector relative to the beam-burst pickoff time is shown in Fig.3. 35 ns time window width was used in the measurement. For a angle the gamma-ray spectrum with the sample in beam, the activation background spectrum with the sample out beam and the background spectrum without sample in beam were in sequence measured. The gamma-ray spectrum at 90^{o} is shown in Fig.4.

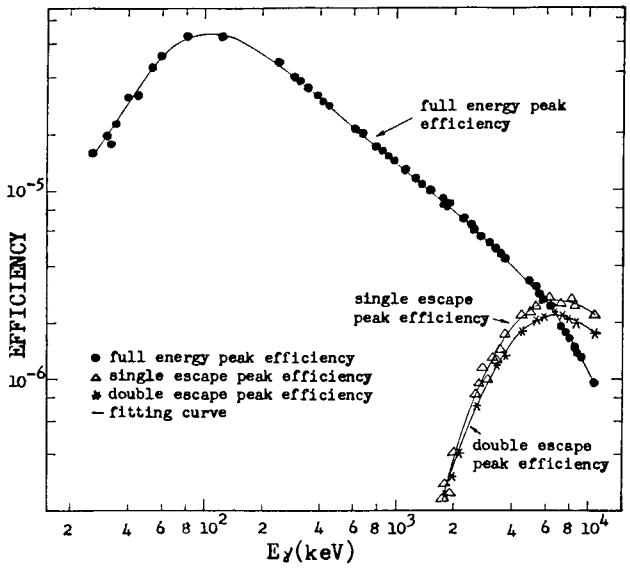

Fig.2 Efficiency curve for coaxial Ge(Li) detector

Data reduction

The details of calculation methods of differential gamma-ray production cross section can be seen in ref.6. In the data reduction of cobalt sample some corrections for neutron and gamma-ray yields were considered as following: the neutron attenuation in the backing and cooling water of the neutron target was estimated to be 2.5%, the neutron and gamma-ray attenuation corrections in the sample are 29.2% and 50.2-628.9% respectively, the neutron elastic and inelastic multiple scattering corrections are 7.9% and 3.7% respectively. The corrections for gamma-ray count loss caused by the threshold of timing channel of the Ge(Li) detector, which should be considered for the gamma-rays with energies less than 180keV, were also made. The calculation methods for above listed corrections can be found in ref.6 and ref.7. The neutron and gamma-ray cross section data of cobalt used in these calculations were taken from ENDF/B-IV and ref.8.

The errors of the differential cross sections were estimated taking account of the uncer-

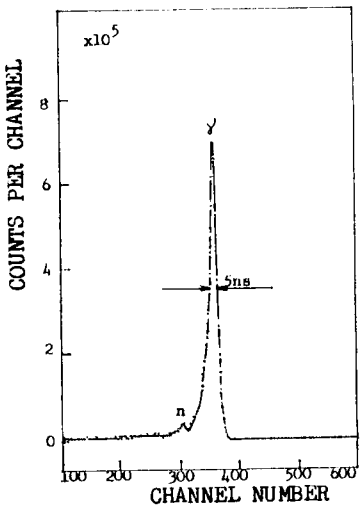

Fig.3 Time spectrum of pulses in the Ge(Li) detector relative to the beam-burst pickoff time

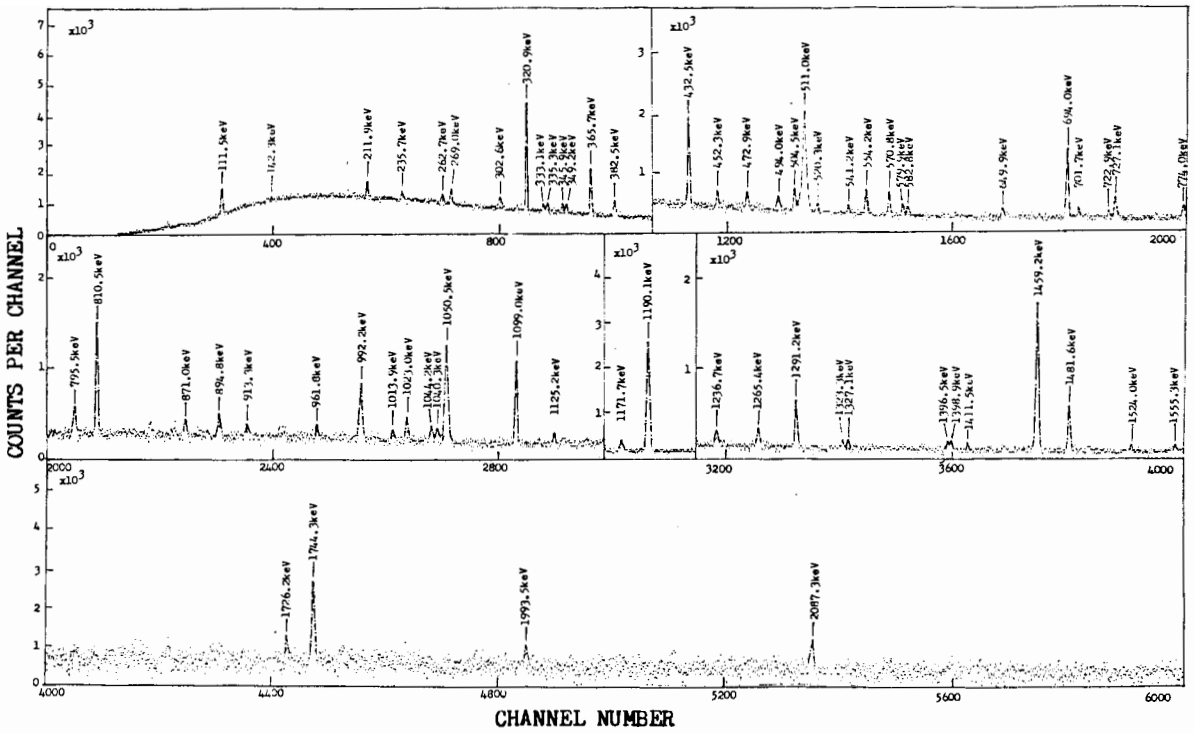

Fig.4 gamma ray spectrum from Co(n,xγ) reactions (En=14.9MeV, θ=90deg.)

tainties in 1. determining the counts $N_\gamma(E_\gamma,\theta)$ in the full energy peak, which depends on the individual gamma-ray peak (1%-100%), 2. determining the neutron flux ϕn incident upon the sample (2%-4%), 3. absolute detection efficiency for full energy peak $\varepsilon(E_\gamma)$ (1.5%-3.0%), 4. the correction factor f (1.0%-3.0%).

Results and discussions

The differential cross sections of 63 gamma-ray lines for the interactions of 14.9MeV neutron with cobalt sample were listed in Table 1. In 110° measurement differential cross section of 111.5keV gamma-ray line is not given because threshold of time channel of the Ge(Li) detector was set uncorrectly. It can be seen from Table 1 that gamma-ray emissions from 14.9 MeV neutron induced $^{59}Co(n,x\gamma)$ reactions are bassically isotropic.

In addition, probable reaction types and transitions of every gamma-ray line besides 1396.5keV line were also given in Table 1 according to ref.9-11, in which some assignments only preliminary and further research is being made.

The neutron inelastic scattering cross sections of 10 energy levels of ^{59}Co in 14.9MeV incident neutron energy were obtained from the results of $(n,n'\gamma)$ reaction in Table 1 and listed in Table 2. In fact, $\sigma n,n'(EL)$ values in Table 2

Table 2. The neutron inelastic scattering cross sections of 10 energy levels of ^{59}Co in 14.9MeV incident neutron energy

EL(keV)	$\sigma n,n'(EL)$(mb)	EL(keV)	$\sigma n,n'(EL)$(mb)
1099.0	50.3±3.0	1744.3	33.8±3.0
1190.1	147.1±7.4	2153.1	88.0±4.4
1291.2	33.2±2.3	2183.0	49.6±3.5
1459.2	115.4±5.8	2204.5	15.6±5.0
1481.6	52.4±3.1	2539.8	32.3±9.6

only are the prescribed maximum because it is possible that the transition gamma-rays with higher energy from higher levels to EL level couldn't be detected because of limitation of the Ge(Li) detector efficiency for the gamma-rays with higher energy.

The total inelastic scattering cross section from 14.9MeV neutron induced $^{59}Co(n,n'\gamma)^{59}Co$ reactions, which were obtained from Table 2, was 617±37mb. Of course, this value is only the prescribed minimum because of similar reason as mentioned above.

REFERENCE

1. J.M. Daniels et al., J. Phys. 46, 1849(1968)

Table 1 Differential gamma-ray production cross sections for 14.9MeV neutron interactions with cobalt sample

Eγ (keV)	Probable Reaction	Transition (keV)	Differential Cross Section (mb/sr)						
			30 deg.	40 deg.	55 deg.	90 deg.	110 deg.	125 deg.	140 deg.
111.5	(n,2n)	111.5-0.0	5.32±0.31	5.31±0.31	5.16±0.30	5.15±0.30		5.54±0.32	5.13±0.31
142.3	(n,α)	2159.1-2016.5	0.546±0.115	0.544±0.100	0.613±0.102	0.561±0.112	0.530±0.106	0.653±0.130	0.581±0.116
211.9	(n,α)	211.9-0.0	1.25±0.19	1.22±0.14	1.31±0.09	1.15±0.11	1.22±0.11	1.04±0.10	1.05±0.09
235.7	(n,2n)	1749.4-1513.7	0.917±0.364	0.680±0.136	0.862±0.170	0.801±0.160	0.500±0.241	0.799±0.160	0.814±0.165
262.7	(n,n')	1744.3-1481.6	0.530±0.186	0.490±0.098	0.492±0.160	0.518±0.076	0.508±0.116	0.465±0.082	0.566±0.097
269.0	(n,n')	1459.1-1190.1	1.14±0.23	1.07±0.11	1.12±0.11	0.890±0.100	0.898±0.107	1.16±0.10	1.01±0.18
302.6	(n,2n)	1378.0-1075.4	0.445±0.142	0.640±0.100	0.611±0.102	0.671±0.086	0.708±0.097	0.676±0.119	0.680±0.090
320.9	(n,2n)	373.7-52.8	9.98±0.50	9.99±0.47	10.83±0.51	10.90±0.51	10.48±0.49	10.54±0.49	10.09±0.31
333.1	(n,n')	3423.7-3090.6	0.532±0.106	0.544±0.410	0.564±0.088	0.644±0.071	0.413±0.083	0.473±0.074	0.658±0.133
335.3	(n,α)	335.3-0.0	0.619±0.124	0.690±0.138	0.571±0.089	0.780±0.085	0.419±0.100	0.708±0.078	0.743±0.180
345.9	(n,2n)	457.4-111.5	0.913±0.146	0.732±0.100	1.02±0.11	0.964±0.100	0.902±0.099	0.959±0.083	0.994±0.075
349.2	(n,2n)	373.7-24.9	0.702±0.112	0.662±0.090	0.814±0.089	0.632±0.090	0.730±0.080	0.944±0.095	0.845±0.064
365.7	(n,2n)	365.7-0.0	5.09±0.27	4.87±0.25	5.16±0.31	4.94±0.25	4.91±0.25	5.23±0.26	5.25±0.18
382.5	(n,n')	1481.6-1099.1	1.17±0.13	1.21±0.12	1.12±0.11	1.25±0.10	1.08±0.11	1.38±0.15	1.31±0.10
432.5	(n,2n)	457.4-24.9	5.28±0.29	5.18±0.26	5.85±0.29	5.59±0.28	5.02±0.25	5.60±0.28	5.41±0.19
452.3	(n,n')	2539.6-2087.3	0.688±0.175	0.646±0.142	0.937±0.132	0.763±0.080	0.896±0.123	1.01±0.12	0.683±0.138
472.9	(n,2n)	1522.3-1049.4	0.972±0.147	1.05±0.20	0.885±0.122	0.956±0.233	0.817±0.105	0.869±0.080	0.935±0.158
494.0	(n,α)	1980.0-1486.0	1.04±0.15	1.06±0.11	0.940±0.103	1.01±0.10	1.02±0.09	0.839±0.086	1.04±0.12
504.5	(n,2n)	1548.6-1044.1	2.01±0.22	2.35±0.24	2.32±0.13	2.17±0.18	2.34±0.16	2.08±0.17	1.85±0.17
520.3	(n,2n)	1757.4-1237.0	0.418±0.113	0.476±0.200	0.471±0.092	0.598±0.123	0.257±0.100	0.549±0.391	0.542±0.159
541.2	(n,n')	5256.0-4714.8	0.300±0.129	0.480±0.100	0.421±0.144	0.425±0.087	0.470±0.115	0.400±0.070	0.555±0.167
554.2	(n,n')	1744.3-1190.1	1.52±0.16	1.63±0.14	1.75±0.15	1.71±0.13	1.54±0.12	1.54±0.11	1.89±0.21
570.8	(n,p)	570.8-0.0	1.86±0.17	1.83±0.11	1.57±0.13	1.72±0.11	1.87±0.14	1.82±0.12	1.89±0.13
579.9	(n,α)	1239.9-660.0	0.873±0.175	0.774±0.235	1.10±0.23	0.919±0.144	1.08±0.17	0.928±0.145	1.01±0.15
582.8	(n,2n)	1039.1-456.3	0.553±0.166	0.495±0.249	0.686±0.174	0.545±0.117	0.667±0.137	0.543±0.111	0.554±0.112
649.9	(n,n')	2712.7-2062.8	0.523±0.110	0.748±0.227	0.603±0.145	0.756±0.120	0.527±0.105	0.666±0.133	0.548±0.338
693.9	(n,n')	2153.1-1459.2	6.18±0.37	6.10±0.31	6.17±0.29	6.12±0.31	6.25±0.32	5.78±0.27	6.27±0.27
701.7	(n,2n)	1075.4-373.7	0.869±0.320	0.761±0.334	0.929±0.282	0.708±0.284	0.682±0.240	0.865±0.262	0.792±0.315
722.9	(n,n')	2204.5-1481.6	0.574±0.100	0.569±0.117	0.609±0.125	0.679±0.172	0.550±0.113	0.704±0.144	0.694±0.209
727.1	(n,2n)	1184.5-457.4	2.36±0.17	1.90±0.21	2.28±0.25	2.22±0.15	2.12±0.23	2.12±0.33	2.12±0.14
774.0	(n,2n)	885.5-111.5	1.09±0.19	1.11±0.12	1.54±0.14	1.47±0.12	1.34±0.15	1.71±0.30	1.30±0.26
795.5	(n,n')	2539.8-1744.3	1.59±0.44	1.55±0.13	1.89±0.16	1.67±0.12	1.81±0.14	1.98±0.15	1.85±0.16
810.5	(n,np)	810.5-0.0	5.79±0.31	5.62±0.27	6.21±0.30	5.64±0.28	5.63±0.30	6.12±0.30	5.71±0.19
871.0	(n,2n)	1236.7-365.7	0.597±0.161	0.788±0.100	1.03±0.12	0.782±0.115	0.757±0.108	1.10±0.11	0.818±0.100
894.8	(n,np)	4139.0-3244.2	0.839±0.168	0.653±0.102	0.827±0.121	0.683±0.140	0.663±0.260	0.854±0.125	0.878±0.177
913.3	(n,n')	2204.5-1291.2							
	(n,2n)	2348.0-1434.7	0.583±0.175	0.548±0.091	0.661±0.135	0.498±0.102	0.791±0.295	0.611±0.095	0.594±0.126
963.0	(n,n')	2153.1-1190.1	0.911±0.137	1.31±0.13	0.771±0.100	0.783±0.110	0.779±0.087	0.827±0.098	0.791±0.100
992.2	(n,n')	2183.0-1190.1	3.92±0.31	4.02±0.26	4.00±0.20	4.16±0.22	4.03±0.24	3.44±0.20	4.08±0.21
1013.9	(n,np)	3890.0-2876.1	0.434±0.217	0.425±0.129	0.426±0.171	0.402±0.162	0.379±0.296	0.327±0.296	0.302±0.151
1023.0	(n,2n)	1075.4-52.8	1.25±0.16	1.03±0.11	1.26±0.11	0.704±0.090	0.962±0.145	1.04±0.10	0.874±0.700
1040.3	(n,2n)	1040.3-0.0	1.41±0.23	1.60±0.13	1.18±0.13	0.999±0.156	1.36±0.21	1.25±0.12	1.22±0.25
1044.2	(n,2n)	1044.2-0.0	0.865±0.173	0.844±0.092	0.794±0.124	0.730±0.121	0.974±0.199	0.933±0.103	0.989±0.199
1050.5	(n,2n)	1075.4-24.9	8.87±0.47	8.69±0.51	8.90±0.45	8.74±0.41	8.63±0.39	8.91±0.42	8.87±0.30
1099.0	(n,n')	1099.0-0.0	5.26±0.27	5.02±0.25	5.51±0.27	5.27±0.25	4.97±0.26	5.23±0.26	5.25±0.21
1125.2	(n,2n)	1236.7-111.5	0.722±0.133	0.702±0.109	0.822±0.097	0.400±0.201	0.503±0.103	0.556±0.168	0.375±0.188
1171.7	(n,n')	4086.3-2914.6	1.81±0.20	1.82±0.13	1.75±0.13	1.81±0.18	1.95±0.36	2.07±0.17	2.08±0.20
1190.1	(n,n')	1190.1-0.0	19.83±0.99	19,93±0.74	19.71±0.90	19.35±0.84	18.57±0.79	18.58±0.82	18.68±0.59
1236.7	(n,2n)	1236.7-0.0	1.39±0.28	1.38±0.28	1.46±0.29	1.22±0.16	1.44±0.25	1.45±0.30	1.32±0.26
1265.4	(n,2n)	1290.3-24.9	1.51±0.16	1.58±0.12	1.43±0.12	1.21±0.11	1.29±0.12	1.14±0.12	1.44±0.15
1291.2	(n,n')	1291.2-0.0	2.89±0.19	3.07±0.16	3.56±0.21	3.35±0.20	3.22±0.19	3.45±0.22	3.22±0.21
1323.3	(n,np)	2133.8-810.5	0.455±0.137	0.456±0.126	0.576±0.100	0.474±0.097	0.458±0.139	0.557±0.280	0.573±0.121
1327.1	(n,2n)	1351.5-24.9	0.593±0.180	0.575±0.184	0.732±0.244	1.11±0.14	0.869±0.220	0.579±0.291	0.976±0.197
1396.5			0.468±0.140	0.482±0.100	0.742±0.225	0.558±0.133	0.637±0.320	0.724±0.363	0.744±0.113
1398.9	(n,α)	1509.4-110.5	0.422±0.136	0.460±0.094	0.585±0.177	0.638±0.154	0.569±0.286	0.672±0.337	0.629±0.127
1411.5	(n,α)	1865.8-454.3	0.435±0.174	0.457±0.139	0.280±0.174	0.315±0.083	0.430±0.216	0.500±0.250	0.624±0.119
1459.2	(n,n')	1459.2-0.0	14.50±0.73	14.26±0.62	15.69±0.69	13.61±0.63	13.45±0.61	14.02±0.63	14.27±0.41
1481.6	(n,n')	1481.6-0.0	4.20±0.28	3.76±0.20	4.68±0.25	4.00±0.21	3.90±0.21	4.10±0.24	3.96±0.29
1524.0	(n,α)	1865.0-341.0	0.308±0.100	0.359±0.109	0.298±0.090	0.319±0.160	0.226±0.113	0.352±0.142	0.426±0.168
1555.3	(n,2n)	1555.3-0.0	0.256±0.297	0.443±0.134	0.626±0.190	0.253±0.140	0.522±0.210	0.505±0.217	0.460±0.276
1726.2	(n,np)	3860.0-2133.8	0.564±0.272	0.635±0.225	0.693±0.279	0.417±0.120	0.494±0.248	0.649±0.234	0.546±0.219
1744.3	(n,n')	1744.3-0.0	2.05±0.22	2.28±0.23	2.30±0.15	2.35±0.14	2.28±0.24	2.47±0.18	2.28±0.28
1993.5	(n,2n)	2105.0-111.5	0.518±0.142	0.465±0.114	0.400±0.320	0.300±0.100	0.376±0.264	0.443±0.222	0.615±0.247
2087.3	(n,n')	2087.3-0.0	0.631±0.148	0.609±0.128	0.779±0.236	0.638±0.150	0.756±0.349	0.557±0.208	0.769±0.232

2. P.T. Guenther et al., Nucl. Sci. Eng. 54, 273(1974)
3. R.V. Leclaire et al., Phys. Rev. c18, 1185 (1978)
4. U. Abbondanno et al., Nucl. Phys. A345, 174(1980)
5. V. Corcalcivc et al., Nucl. Phys. A307, 445(1978)
6. Zhou Hongyu et al., INDC(CPR) 010/L (1986)
7. Zhou Hongyu et al., A United Method of Calculating Neutron Flux Attenuation and Gamma-ray Self-Absorption in a Large Cylindrical Sample, Contributed Paper to This Conference(1988)
8. Liu Yingzang et al., Decay Scheme, Atomic Energy Publishing House, 1982, p. 470-471
9. D.M. Lederer et al., Table of Isotopes, U.S. A., John Wiley & Sons, Inc., 1978, P. 160-172
10. P. Andersson et al., Nucl. Data Sheets 39, 641(1983)
11. L.k. Peker, Nucl. Data Sheets 42, 457(1984)

*The work supported by the National Natural Science Foundation of China and Ministry of Nuclear Industry of China